King's Research Portal

Link to publication record in King's Research Portal

Clinical significance of hypoxia in nasopharyngeal carcinoma with a focus on existing and novel hypoxia molecular imaging

Connie Yip[1,2], Gary J. R. Cook[1,3], Joseph Wee[2], Kam Weng Fong[2], Terence Tan[2], Vicky Goh[1,4]

[1]Department of Cancer Imaging, Division of Imaging Sciences & Biomedical Engineering, King's College London, St Thomas' Hospital, London SE1 7EH, UK; [2]Department of Radiation Oncology, National Cancer Centre, Singapore; [3]Clinical PET Imaging Centre, [4]Department of Radiology, Guy's and St Thomas' NHS Foundation Trust, St Thomas' Hospital, London SE1 7EH, UK

Contributions: (I) Conception and design: C Yip; (II) Administrative support: C Yip, V Goh, GJ Cook; (III) Provision of study materials or patients: None; (IV) Collection and assembly of data: C Yip; (V) Data analysis and interpretation: C Yip; (VI) Manuscript writing: All authors; (VII) Final approval of manuscript: All authors.

Correspondence to: Dr. Connie Yip. Department of Radiology, Level 1, Lambeth Wing, St Thomas' Hospital, Lambeth Palace Road, London SE1 7EH, UK. Email: connie.yip@kcl.ac.uk.

Abstract: Locally advanced nasopharyngeal carcinoma (NPC) is still associated with significant locoregional failure and poor overall survival (OS) after chemoradiation. The maximal therapeutic effect of conventional chemotherapy combined with radiation may have been reached and there is a clinical need to identify additional adverse prognostic factors that could be targeted therapeutically. Hypoxia, a known prognostic factor in head and neck cancers is an attractive target in NPC with various treatment strategies available such as hypoxic cell sensitisers/cytotoxins and increasing intratumoral oxygen delivery, to overcome the poorer outcomes associated with this phenotype. Thus, we aim to review the clinical significance of hypoxia as well as the current and future of molecular hypoxia imaging in NPC.

Keywords: Nasopharyngeal carcinoma (NPC); hypoxia; positron emission tomography (PET); single photon emission computed tomography (SPECT); magnetic resonance imaging (MRI)

Introduction

Nasopharyngeal carcinoma (NPC) is uncommon with approximately 87,000 new cases which accounted for 0.6% of all cancers diagnosed worldwide in 2012 (1). The majority of cases are found in east and southeast Asia, north Africa, Middle East and the Arctic (2). NPC is a distinctive cancer that differs from other head and neck malignancies in terms of its pathogenesis, clinical progression and management strategy (3,4). It is classified into three pathological subtypes: keratinising squamous cell carcinoma (SCC), nonkeratinising carcinoma (which comprises differentiated and undifferentiated types) and basaloid SCC (5). The Epstein-Barr virus (EBV) is implicated in the development of NPC, particularly in the endemic non-keratinising subtype with specific expression of several latent genes. These include the EBV nuclear antigen (*EBNA1*), latent membrane proteins (*LMP1*, *LMP2*) and EBV encoded noncoding RNAs (EBERs) in contrast to the conventional risk factors associated with head and neck SCC (HNSCC) (6,7).

Definitive (chemo)radiotherapy is the primary treatment modality in NPC with little role for surgical intervention apart from in the salvage setting. There have been few significant breakthroughs in the management of this disease since the introduction of concurrent chemoradiation in those with advanced disease which yielded 5-year overall survival (OS) rates between 67–81% and locoregional control rates of 78–90% (3). Efforts to improve these figures by means of induction chemotherapy or altered radiotherapy fractionation have been disappointing (8,9). Perhaps a more personalised and targeted approach is required to improve clinical outcomes in NPC.

Intratumoral hypoxia is an important negative prognostic factor in HNSCC (10,11). However, most if not all of these studies excluded patients with NPC and thus, the actual prevalence of hypoxia in the NPC population is still unclear. Intratumoral hypoxia is an important predictive factor for radiotherapy, and to a lesser extent, chemotherapy response (12). This could be particularly pertinent in the predominantly non-surgical management of NPC. Intratumoral oxygenation is a dynamic process which is dependent on cellular extraction or utilisation of oxygen, oxygen transport capacity, vascular perfusion and interstitial pressure (13). Conventional classification of acute hypoxia due to perfusion changes, chronic hypoxia due to increased perfusion distance in larger tumours and hypoxaemic hypoxia due to reduced oxygen transport capacity are not mutually exclusive and it is extremely difficult to clinically establish the contribution of each component to the overall tumour oxygenation status (14). The exact partial oxygen pressure (pO_2) level which defines hypoxia is dependent on the tissue or tumour type but should be the critical level that impairs normal cellular function (15). This critical pO_2 level is usually between 8 to 10 mmHg in most tumour types but the pO_2 level which causes treatment resistance could be higher and again, varies with the treatment modality involved (13). This review aims to assess the prevalence and relevance of hypoxia in NPC and to evaluate the role of non-invasive molecular hypoxia imaging in this disease.

Evidence of hypoxia in NPC

Overall, there is scant evidence in the published literature regarding the actual prevalence of hypoxia in NPC. The very limited pO_2 data that is available suggests that NPC tumours can be hypoxic but what proportion of nasopharyngeal tumours is indeed hypoxic is unclear. The data from pathological hypoxia assessment in NPC suggests that up to half of these tumours have some degree of hypoxia. However, whether these endogenous markers are true reflections of intratumoral oxygenation status is still debatable. In HNSCC, the proportion of hypoxic tumours can be as high as 58% and tumour oxygenation did not seem to differ between primary and nodal metastases (14,16). However, in view of the different pathogenesis and risk factors implicated in NPC, particularly the endemic form, and HNSCC which has a higher proportion of smokers and drinkers and hence, greater risk of vasculopathy, the prevalence of extreme hypoxia in NPC may be lower compared to SCC. Nonetheless, hypoxia in NPC may still

be a significant problem particularly in those with bulky locoregional disease.

To date, there is no published study that examined the prevalence of intratumoral oxygenation in NPC by means of pO_2 measurement. A number of studies have evaluated the prevalence of hypoxia using polarographic needle electrode histography in head and neck cancers which included predominantly SCCs (17-25). Polarographic needle electrode histography is an automated system which uses a 250–350 μm oxygen-sensitive probe which is inserted into the tumour and progresses in a stepwise pattern over a predetermined distance, enabling multiple real-time pO_2 sampling within the tumour with fine spatial resolution (14,19). This method is considered the gold standard in intratumoral oxygenation measurement although it has several important limitations. Firstly, repeated assessment during therapy is difficult due to its invasive nature and it is not suitable for deep seated tumours. It cannot distinguish viable tumours from necrotic tissue and thus, will require additional imaging or pathological assessment for this purpose.

Other methods of tumour hypoxia assessment are quantification of downstream endogenous genomic or proteomic markers involved in hypoxia-induced cellular signalling such as hypoxia-inducible factors (HIFs), carbonic anhydrase IX (CA-IX), glucose transporter 1 (GLUT1) and osteopontin (OPN). A noteworthy study investigated the *in vitro* hypoxic induction of HIF-1α, HIF-2α, CA-IX and vascular endothelial growth factor (VEGF) at the mRNA and proteomic levels in four NPC cell lines representing all NPC subtypes: keratinising SCC (HK1), undifferentiated carcinoma (C666-1) and poorly differentiated carcinoma (HONE-1, CNE-2) (26). HIF-1α expression was increased after 16 hours of hypoxia exposure in all four cell lines. Expression of CA-IX was also increased in 3 cell lines but not C666-1. However, VEGF expression was only increased after 24 hours of hypoxia exposure in C666-1, HONE1 and CNE-2 cells. HIF-2α expression was not increased in any of the cell lines following hypoxia exposure. The group also performed microarray analysis profiling hypoxic and normoxic gene expressions in HONE-1 and CNE-2 cells which showed that 4.6–7.6% of measured transcripts were regulated by hypoxia. Overall, these results suggest that the transcription and translation of hypoxic genes are probably dependent on both tumour type and duration of hypoxia exposure. OPN is a phosphoglycoprotein that is found in tumours, some normal tissues and body fluids (27). It is implicated in tumour invasion, migration and metastasis.

Research has mostly concentrated on the role of plasma OPN as a hypoxic biomarker which is thought to be shed primarily from tumour cells (28). However, this assumption should be reconsidered as plasma OPN may be derived from other tissues such as bones, immune and endothelial cells (27). In fact, OPN expression was restricted to tumour-infiltrating macrophages, not tumour cells in pancreatic adenocarcinoma (29). Whether plasma and intratumoral OPN levels can be used interchangeably as a hypoxic biomarker, if indeed it is one, could perhaps be answered by a study by Nordsmark *et al.* which failed to show any correlation between the blood and intratumoral OPN levels (30). In addition, OPN secretion was found to be cell line dependent and increased by reoxygenation, rather than hypoxia exposure in an *in vitro* study (31). These findings were supported by an *in vivo* study which found that intratumoral and plasma OPN levels were dependent on the strains of mice and tumour models, and OPN levels were increased by reoxygenation rather than prolonged hypoxia exposure (32). Despite the uncertainty of OPN as a true hypoxic biomarker, plasma OPN has been shown to be a significant prognostic marker in HNSCC (28,33). Although immunohistochemistry is easy to perform in clinical practice, these endogenous markers are not purely specific to hypoxia and may be affected by other biological processes in the tumour microenvironment (34). Pathological assessment is also not representative of what is happening at the whole tumour level due to sampling limitation. The cost of hypoxic genomic analysis prohibits its routine use in clinical practice at present although this may change in the future. Moreover, one cannot assume that hypoxia-induced gene expression or repression will lead to corresponding proteomic changes (35), which adds another layer of complexity in applying genomic or downstream proteomic hypoxic biomarkers to direct treatment in the clinic. In view of the potential importance of hypoxia in NPC, we will review the available evidence of hypoxia as measured using polarographic needle electrode system and pathological assessment in NPC.

A German group showed that pO_2 status in primary and nodal tumours were not significantly different in 15 HNSCC patients who had simultaneous pO_2 sampling of their primary and nodal tumours (17). The study included one patient with nasopharyngeal SCC who had nodal pO_2 sampling only. The median nodal pO_2 for this patient was 13.5 mmHg and hypoxic fraction (HF) which was defined as the percentage of pO_2 readings with values below 5.0 mmHg ($HF_{5.0}$) was 0%. Brizel *et al.* acquired pretreatment pO_2 measurements from 28 locally advanced HNSCC cases which included one patient with a nasopharyngeal primary (21). In contrast to the previous study, the median nodal pO_2 for this patient was 3.8 mmHg and $HF_{5.0}$ was 36%. An update of the latter study (n=63) included one additional NPC primary but no individual pO_2 data were available (22). Adam *et al.* measured tumour oxygenation in 37 patients with head and neck malignancies, seven of whom had received prior treatment (18). Nodal pO_2 measurement was acquired in one patient with nasopharyngeal SCC that was found to be very hypoxic: median pO_2 1.8 mmHg, $HF_{2.5}$ 81%, $HF_{5.0}$ 94% and $HF_{10.0}$ 96%. Several other studies included a small number of NPC patients but did not provide individual patient data regarding the pO_2 measurements (20,23). Of interest, one of these studies evaluated the relationship between computed tomography (CT) derived tumour volume and hypoxic tumour volume as defined using pO_2 measurements (20). The latter assessment was performed mainly on nodal masses. Two out of 125 patients had nasopharyngeal SCC. The study found that CT tumour volumes positively correlated with hypoxic volumes (HVs).

There are more published studies that evaluated pathological hypoxic markers in NPC (*Table 1*) (36-43). Most studies evaluated HIF-1α expression which was found in 32–83% of patients (*Table 1*). One study found that 57% of nasopharyngeal tumours expressed CA-IX (37) and VEGF expression was found in 41–80% (36,37,41,42). However, it should be noted that VEGF is not strictly a hypoxic marker, but rather an angiogenic marker whose expression is upregulated by HIF-1 (46). Patients with NPC were found to have higher levels of plasma OPN compared to normal controls (mean 185 *vs.* 76 ng/mL, P=0.001) but no correlation to oxygenation status was made (44). In a separate study, plasma OPN did not differ between patients with NPC and normal controls (45).

Hypoxia as a prognostic biomarker

To our knowledge, there is no published study which evaluated invasive pO_2 status as a prognostic marker in NPC. On the other hand, pathological hypoxic biomarkers have been studied more extensively in NPC (*Table 2*) (36-40, 42,47). The majority of these studies investigated HIF-1α. All but one study (36) included predominantly the undifferentiated subtype. On an individual study level, the association between HIF-1α and locoregional control, disease-free survival (DFS) and OS were rather poor with

Page 4 of 24

Yip et al. Molecular imaging of hypoxia in NPC

Table 1 Studies that evaluated the prevalence of pathological hypoxia markers in NPC

Study	No. of patients	Tumour subtype	Tumour stage	Results			
				HIF-1α	CA-IX	VEGF	OPN
Xueguan et al. (36)	59	Nonkeratinising carcinoma	II–IV	68%	—	49%	—
Hui et al. (37)	90	Nonkeratinising carcinoma	II–IV	58%	57%	60%	—
Kitagawa et al. (38)	74	Nonkeratinising carcinoma (n=68), keratinising SCC (n=6)	I–IV	36%	—	—	—
Wan et al. (39)	144	Nonkeratinising carcinoma	III–IV	46%	—	—	—
Shou et al. (40)	60	Nonkeratinising carcinoma	I–IV	70%; normal NPC epithelium: 46%	—	—	—
Guang-Wu et al. (41)	73	Nonkeratinising carcinoma	I–IV	—	—	80%	—
Chan et al. (42)	78	Nonkeratinising carcinoma	II–IV	32%	—	41%	—
Benders et al. (43)	21	n/a	n/a	83%	—	—	—
Wong et al. (44)	72+72 controls	Nonkeratinising carcinoma	I–IV	—	—	—	NPC vs. normal: mean 185 vs. 76 ng/mL
Hui et al. (45)	44+29 controls + 22 head & neck cancers	Nonkeratinising carcinoma	I–IV	—	—	—	NPC vs. normal: mean 705 vs. 523 ng/mL (P=0.0073); HNN: mean 728 ng/mL

NPC, nasopharyngeal carcinoma; HIF-1α, hypoxia-inducible factor-1α; CA-IX, carbonic anhydrase IX; VEGF, vascular endothelial growth factor; OPN, osteopontin; SCC, squamous cell carcinoma; n/a, not available.

the 95% confidence intervals (CI) crossing the 1.00 cut-off. Furthermore, its prognostic significance was lost after adjusting for confounding factors in multivariate analyses. Nonetheless, the prognostic values of HIF-1α and HIF-2α in head and neck cancers were supported in a recent systematic review (48). A subset analysis included five studies (n=445) which looked solely at HIF-1α expression in NPC. Overexpression of HIF-1α was associated with inferior OS in all patients and also in the NPC subgroup (HR 2.07, 95% CI, 1.23–3.49). Fewer studies evaluated the prognostic role of CA-IX, VEGF and/or OPN but similar to HIF-1α, their prognostic significance was not conclusive in these retrospective studies (*Table 2*). Perhaps predictably, a combination of hypoxic, or hypoxic and angiogenic factors appeared to provide a more robust prognostic stratification (37,42).

Hypoxia imaging in NPC

Intuitively, a proportion of nasopharyngeal tumours will be hypoxic based on the extrapolation of current evidence in the HNSCC population. The degree of intratumoral hypoxia is likely to be greater with increasing tumour bulk. Besides being a potential prognostic biomarker, it would also be clinically beneficial if we could assess changes in intratumoral oxygenation during and after nonsurgical therapy, allowing us to intensify treatment, where appropriate. Both of the commonly used methods in hypoxia assessment, namely invasive pO_2 sampling and immunohistochemistry are associated with limitations. An ideal hypoxic biomarker should be hypoxia-specific with selective cellular uptake at a clinically relevant pO_2 level, reproducible, non-toxic and cost effective. While it is unlikely that any biomarker will fulfil all of these

Table 2 Studies that evaluated the prognostic role of hypoxia biomarker in NPC

Study	No. of patients	Tumour subtype	Stage	Treatment	Prognostic markers	Locoregional control	Disease-free survival	Overall survival
Xueguan et al. (36)	59	Nonkeratinising carcinoma	II–IV	RT + carbogen + nicotinamide	HIF-1α, VEGF	Univariate (5-yr rates): HIF-1α (+) vs. (–): 88% vs. 95% (P=0.35); VEGF (+) vs. (–): 86% vs. 92% (P=0.32). Multivariate: n/a	Univariate (5-yr rates): HIF-1α (+) vs. (–): 65% vs. 90% (P=0.04); VEGF (+) vs. (–): 59% vs. 87% (P=0.01). Multivariate: HIF-1α: HR 2.48, 95% CI, 0.50–12.29 (P=0.27) VEGF: HR 3.14, 95% CI, 0.94–10.51 (P=0.06)	Univariate (5-yr rates): HIF-1α (+) vs. (–): 75% vs. 100% (P=0.02); VEGF (+) vs. (–): 72% vs. 93% (P=0.03). Multivariate: HIF-1α: HR 99.80, 95% CI, 0–220.12 (P=0.96); VEGF: HR 3.15, 95% CI, 0.64–15.63 (P=0.16)
Hui et al. (37)	90	Nonkeratinising carcinoma	II–IV	CRT	HIF-1α, CA-IX, VEGF	n/a	Univariate: HIF-1α: RR 1.72, 95% CI, 0.87–3.39 (P=0.12); CA-IX: RR 1.28, 95% CI, 0.65–2.52 (P=0.48); VEGF: RR 1.52, 95% CI, 0.76–3.04 (P=0.24); HIF-1α + CA-IX: RR 2.06, 95% CI, 1.00–4.23 (P=0.04); HIF-1α + CA-IX + VEGF: RR 2.87, 95% CI, 1.25–6.59 (P=0.01). Multivariate: HIF-1α + CA-IX + VEGF: P=0.022	Univariate: HIF-1α: RR 2.12, 95% CI, 0.96–4.70 (P=0.06); CA-IX: RR 1.39, 95% CI, 0.64–3.01 (P=0.40); VEGF: RR 1.12, 95% CI, 0.52–2.41 (P=0.78); HIF-1α + CA-IX: RR 2.13, 95% CI, 0.95–4.80 (P=0.06); HIF-1α + CA-IX + VEGF: RR 2.22, 95% CI, 0.84–5.88 (P=0.10). Multivariate: n/a
Kitagawa et al. (38)	74	Nonkeratinising carcinoma [68], keratinising SCC [6]	I–IV	CRT or RT	HIF-1α	n/a	n/a	Univariate: HIF-1α: HR 2.06, 95% CI, 1.13–3.74 (P=0.01). Multivariate: HIF-1α: HR 1.99, 95% CI, 1.01–3.90 (P=0.04)
Wan et al. (39)	144	Nonkeratinising carcinoma	III–IV	CRT	HIF-1α	Univariate: HIF-1α: P=0.244. Multivariate: HIF-1α: HR 1.574, 95% CI, 0.657–3.770 (P=0.309)	Univariate: HIF-1α: P=0.040. Multivariate: HIF-1α: HR 1.601, 95% CI, 0.918–2.790 (P=0.097)	Univariate: HIF-1α: P=0.226. Multivariate: HIF-1α: HR 1.290, 95% CI, 0.693–2.401 (P=0.422)

Table 2 (*continued*)

Page 6 of 24

Yip et al. Molecular imaging of hypoxia in NPC

Table 2 (*continued*)

Study	No. of patients	Tumour subtype	Stage	Treatment	Prognostic markers	Locoregional control	Disease-free survival	Overall survival
Shou et al. (40)	60	Nonkeratinising carcinoma	I–IV	CRT or RT	HIF-1α	n/a	n/a	Univariate: HIF-1α: RR 4.192, 95% CI, 1.244–14.124 (P=0.021). Multivariate: not significant but no hazard ratios were given
Hui et al. (45)	31	Nonkeratinising carcinoma	I–IV	CRT or RT	OPN	Dichotomised OPN levels: > median 545 ng/mL vs. s median. All patients: CR rates: 40% vs. 88% (P=0.009), CRT-treated group (n=21): CR rates: 20% vs. 82% (P=0.009)	n/a	n/a
Chan et al. (42)	78	Nonkeratinising carcinoma	II–IV	CRT or RT	HIF-1α, VEGF, COX-2	Univariate: HIF-1α + COX-2: P=0.004 (local) and P=0.007 (regional); VEGF + COX-2: P<0.001 (local). Multivariate: HIF-1α + VEGF: local: HR 9.354, 95% CI, 3.019–28.14 (P<0.001); regional: HR 20.72, 95% CI, 4.154–103.4 (P<0.001)	Univariate: HIF-1α + COX-2: P=0.046. Multivariate: HIF-1α + VEGF: HR 2.922, 95% CI, 1.428–5.982 (P=0.003)	Univariate: No significant factors. Multivariate: no significant factors
Koukourakis et al. (47)	7 (+191 HNSCC)	Keratinising SCC	I–IV	Hyperfractionated RT or conventional RT	HIF-2α, CA-IX	Univariate (5-yr rates): HIF-2α (+) vs. (–): 42% vs. 64% (P=0.002); CA-IX (+) vs. (–): 41% vs. 65% (P=0.004)	n/a	Univariate (5-yr rates): HIF-2α (+) vs. (–): 39% vs. 61% (P=0.0004); CA-IX (+) vs. (–): 39% vs. 60% (P=0.002)

NPC, nasopharyngeal carcinoma; SCC, squamous cell carcinoma; HNSCC, head and neck squamous cell carcinoma; RT, radiotherapy; CRT, chemoradiation; HIF-1α, hypoxia-inducible factor-1α; CA-IX, carbonic anhydrase-IX; VEGF, vascular endothelial growth factor; OPN, osteopontin; CR, complete response; COX-2, cyclooxygenase-2; n/a, not available.

requirements, hypoxia imaging has gained considerable attention over recent years as it has the potential to fulfil most of these requirements. One of the major advantages of hypoxia imaging is its ability to acquire multiple high resolution 3-dimensional data over the regions of interest at different time points. We will review the available hypoxia imaging modalities which have been applied in NPC and novel imaging techniques that have the potential to be used in this disease. We will also discuss some relevant HNSCC studies when data on NPC is unavailable.

Positron emission tomography (PET)

Nitroimidazoles

There are several derivatives of nitroimidazole PET tracers in the clinical and research setting. In general, nitroimidazole enters the cell by passive diffusion and is reduced by nitroreductase enzymes to form RNO_2 radicals. In the presence of oxygen, these radicals are rapidly reoxidised and the parent compound diffuses out of the cell. In hypoxic cells, the radical is further reduced and then binds to intracellular macromolecules, irreversibly trapping it within the cell (49). Retention of nitroimidazoles only occurs in viable cells with functional nitroreductase enzymes but not in necrotic cells (50) and is increased when pO_2 falls below 10 mmHg (51). Most of the nitroimidazoles are labelled with fluorine-18 [^{18}F] which has a physical half-life ($T_{1/2}$) of 109.8 minutes (52).

[^{18}F]Fluoromisonidazole ([^{18}F]FMISO)

[^{18}F]FMISO is the most extensively investigated nitroimidazole PET tracer. However, it is associated with low hypoxia-specific tissue accumulation leading to poor image contrast between hypoxic and normoxic tissues. There is slow non-hypoxic cellular washout and typically requires a 2–4 hour interval between tracer injection and image acquisition, after which the [^{18}F] would have decayed by more than one half-life (53). Quantification of [^{18}F]FMISO uptake has been performed using tumour-to-background ratios (TBaR) such as tumour-to-blood (TBR), tumour-to-muscle (TMR), as well as standardised uptake value (SUV), HF or HV. [^{18}F]FMISO TBR at 2 hours post injection (TBR$_{2h}$) >1.2 is generally regarded as hypoxia-specific uptake although many studies have also used the cut off of 1.4 (54). There are no definitive cut offs for TMR and SUV for [^{18}F]FMISO or any of the other nitromidazoles.

There are many published correlative studies which attempted to examine the relationship between [^{18}F]FMISO uptake with pO_2 measurements and pathological evidence of hypoxia both in the preclinical and clinical setting (*Table 3*) (55-69). Despite the relatively larger number of correlative studies compared to other hypoxic radiotracers, there is an overall weak correlation between [^{18}F]FMISO uptake and pO_2 measurement (54,70). However, better correlation was observed between [^{18}F]FMISO uptake and pimonidazole staining, an exogenous hypoxic marker, in the preclinical setting (58,59,61). Both [^{18}F]FMISO and pimonidazole are members of the nitroimidazole family, thus have similar hypoxia retention mechanisms. Uptake probably depends on a combination of acute and chronic hypoxia as both markers have to be administered several hours prior to their evaluations compared to electrode pO_2 measurement which is instantaneous, and thus may be influenced more by acute hypoxia.

An early study by Yeh *et al.* evaluated the use of [^{18}F]FMISO PET to detect hypoxia in NPC (71). The study included 24 patients with NPC and 12 normal controls. A total of 370 MBq [^{18}F]FMISO was injected intravenously and two acquisition protocols were used. The long protocol consisted of dynamic acquisition from 0 to 180 minutes and the short protocol involved two 30-minutes scan at 2 hours post injection. The authors compared TMR$_{2h}$ and normal nasopharynx-to-muscle ratio (NMR) in NPC patients and controls, respectively. Tumour retention of [^{18}F]FMISO was observed after 30 minutes which persisted until 3 hours post injection. As expected, primary tumoral (mean TMR$_{2h}$ of 2.56±1.50) and nodal uptake (1.35±0.51) of [^{18}F]FMISO were higher than that of normal nasopharynx (mean NMR 0.96±0.014, P<0.005). Applying a TMR$_{2h}$ threshold of 1.24, all primary tumours were found to be hypoxic but only 58% of cervical nodal metastases were hypoxic. Their results also suggested that there was a difference in [^{18}F]FMISO uptake between the different tumour subtypes. Non-keratinised carcinoma (n=13) was associated with higher TMR$_{2h}$ compared to undifferentiated carcinoma (n=10) (3.22±1.80 *vs.* 1.72±0.50, P<0.05). There were too few keratinised carcinomas in this study to allow similar comparison.

[^{18}F]FMISO PET has been evaluated as a potential prognostic biomarker as well as a treatment response and radiotherapy planning tool in HNSCC. Several studies have shown that [^{18}F]FMISO uptake is associated with a poor prognosis in HNSCC (72-76) although others have found no such association (77,78). To our knowledge, there is only one similar study in NPC which was published as an abstract (79). This study included 40 patients who had

Page 8 of 24

Yip et al. Molecular imaging of hypoxia in NPC

Table 3 Studies which compared [18F]FMISO uptake against pO2 measurements and hypoxia immunohistochemistry

Study	Study type	Tumour type	Hypoxic markers	PET parameters	Results
Bentzen et al. (55)	Preclinical	C3H mammary carcinoma	Polarographic pO2 measurement	HF = ratio of radioactivity between tumour & reference tissue between 225–300 minutes pi	Autoradiography showed decreased [18F]FMISO uptake in mice breathing Carbogen compared to normal air. No correlations between pO2 measurements and [18F]FMISO uptake
O'Donoghue et al. (56)	Preclinical	R3327-AT anaplastic prostate adenocarcinoma	OxyLite fibreoptic probe which converts optical fluorescence SI to pO2 values	Qualitative assessment of [18F]FMISO images at 30 minutes to 4 hours pi	Spatial localisation of [18F]FMISO uptake corresponded to areas of low pO2
Chang et al. (57)	Preclinical	R3327-AT	OxyLite fibreoptic probe	SI at 2 hours pi	[18F]FMISO SI was negatively correlated with pO2 (r=−0.60–0.83)
Dubois et al. (58)	Preclinical	R1 rhabdomyosarcoma	Pimonidazole, CA-IX	HF = ratio of tumour-to-heart activity defined using thresholds ranging from 1.2–3.0 at 2 hours pi	Significant correlations observed between pimonidazole & [18F]FMISO volume (r=0.9066, P=0.0001) and CA-IX & [18F]FMISO volume (r=0.8636, P=0.0006)
Troost et al. (59)	Preclinical	Human HNSCC (SCCNij3), human glioblastoma (E102, E106)	Pimonidazole	Autoradiography	Weak pixel-by-pixel correlations between pimonidazole staining & mean [18F]FMISO SI (r²=0.07–0.48)
Troost et al. (60)	Preclinical	Nine human HNSCC & one mucoepidermoid carcinoma	Pimonidazole	Autoradiography	Weak pixel-by-pixel correlations between pimonidazole & [18F]FMISO images (r=0.04–0.19)
Carlin et al. (61)	Preclinical	Human HNSCC (SQ20b) (used in all four tracer experiments). Human colon cancer (HCT116 & HT29) (used only in [64Cu]ATSM experiments). Images acquired at 80–90 minutes pi	Pimonidazole, CA-IX, Hoechst 33342	4 tracers evaluated: [18F]FMISO, [18F]FAZA, [18F]HX4 & [64Cu]ATSM. Autoradiography	Qualitative: areas of high uptake of 2-nitroimidazoles corresponded to regions of high pimonidazole & CA-IX staining, and low Hoechst 33342 staining; weak-moderate positive correlations between 2-nitroimidazole uptake and pimonidazole & CA-IX staining and negative correlation with Hoechst 33342 Quantitative: weak correlations between pimonidazole & 2-nitroimidazoles (r=0.122–0.398); weak-moderate correlations between CA-IX & 2-nitroimidazoles (r=0.140–0.433); weak-moderate correlations between Hoechst 33342 & 2-nitroimidazoles (r=0.004–0.424)
Hueting et al. 2014 (62)	Preclinical	EMT6 mouse mammary cell line, CaNT murine adenocarcinoma	EF5	Autoradiography	Good correlation between [18F]FMISO uptake & EF5 (r>0.8)

Table 3 (*continued*)

Table 3 (*continued*)

Study	Study type	Tumour type	Hypoxic markers	PET parameters	Results
Zimny et al. (63)	Clinical	HNSCC (n=22), Hodgkin's lymphoma (n=1), lymphoepithelial cancer (n=1)	Polarographic pO_2 measurement	TMR_{2hr} & TBR_{2hr}	Moderate correlations between pO_2 HF ≤2.5 (r=0.50)/5.0 mmHg (r=0.54) and [^{18}F]FMISO TMR. Correlations were improved after exclusion of 2 outliers with mainly necrotic tumours (r=0.78–0.80)
Gagel et al. (64)	Clinical	HNSCC (n=20)	Polarographic pO_2 measurement	TMR_{2hr} & TBR_{2hr}	Good correlations between pO_2 HF (r=0.703–0.757), & median (r=−0.589) and mean pO_2 (r=−0.582) with [^{18}F]FMISO TMR. Weaker correlations between pO_2 HF (r=0.435–0.478), median (r=−0.278) and mean pO_2 (r=−0.272) with [^{18}F]FMISO TBR
Mortensen et al. (65)	Clinical	HNSCC (n=9), soft-tissue sarcoma (n=5), benign soft tissue tumours (n=4)	Polarographic pO_2 measurement	TMR at 150–249 minutes pi	No significant correlation between pO_2 measurements and [^{18}F]FMISO uptake
Cherk et al. (66)	Clinical	NSCLC (n=17)	HIF-1α, GLUT1	SUV_{max} at 2 hours pi	No significant correlations between SUV_{max} & HIF-1α/GLUT1 expressions
Norikane et al. (67)	Clinical	Head & neck (n=24) including 2 NPC	HIF-1α	TBR_{2hr}	Weak correlation between HF & HIF-1α staining (r=0.40). No correlation between TBR & HIF-1α staining (r=0.09)
Sato et al. (68)	Clinical	HNSCC (n=23)	HIF-1α	SUV_{max} at 4 hours pi	No significant correlation between SUV_{max} & HIF-1α expression
Kawai et al. (69)	Clinical	High grade gliomas (n=48)	HIF-1α	TBR_{2hr}	No significant correlation between TBR & HIF-1α expression

HF, hypoxic fraction; pi, post injection; SI, signal intensity; HNSCC, head and neck squamous cell carcinoma; TMR, tumour-to-muscle ratio; TBR, tumour-to-blood ratio; SUV, standardised uptake value; HIF-1α, hypoxia-inducible factor-1α; CA-IX, carbonic anhydrase-IX; GLUT1, glucose transporter 1; NSCLC, non-small cell lung cancer.

Page 10 of 24

Yip et al. Molecular imaging of hypoxia in NPC

pretreatment [^{18}F]FMISO and [^{18}F]FDG PET. Patients were injected with 370 MBq of [^{18}F]FMISO and PET was acquired at 2 hours post injection. Hypoxia was defined as [^{18}F]FMISO TMR$_{2hr}$ >1.24. Overall, 75% of all patients had baseline PET-defined hypoxia. Fewer number of complete responders (n=25) had baseline hypoxia compared to non-responders or those with disease relapse (64% *vs.* 93%).

In contrast, there are more studies which utilised [^{18}F] FMISO PET in NPC radiotherapy planning. A Korean group performed a dose escalation radiotherapy planning study in a small cohort of head and neck malignancies (80). Six out of eight patients had locally advanced NPC. Static PET image acquisition was performed at 2 and 4 hours post intravenous injection of approximately 740 MBq of [^{18}F]FMISO. Interestingly, the group used tumour-to-cerebellum ratio (TCR) ≥1.3 to define hypoxic gross tumour volume (GTV$_h$) instead of TMR which they postulated could be affected by cervical muscle strain secondary to anxiety or stress. A 3 mm margin was applied to GTV$_h$ to generate hypoxic planning target volume (PTV$_h$). Dose escalation to the GTV$_h$ from the standard 72 to 84 Gy delivered over 30 fractions was simulated using simultaneous-integrated boost intensity-modulated radiotherapy (SIB IMRT). Mean intratumoral [^{18}F]FMISO SUV maximum (SUV$_{max}$) was found to be 2.1±0.9 and the mean GTV$_h$-to-standard GTV ratio was 16.3%±24.7%. Dose escalation was not feasible in two NPC patients with T4N2 disease due to brainstem and spinal cord tolerance, respectively. Dose escalation of up to 78–84 Gy was feasible in the other patients.

A Japanese group investigated the radiotherapy planning and prognostic roles of [^{18}F]FMISO acquired on a new PET/CT scanner using lutetium oxyorthosilicate scintillation detectors and extended field of view which provided better image contrast, with images acquired on a conventional PET/CT scanner with bismuth germanium oxide scintillation detectors in 16 patients with NPC (81). The patients were injected with 400 MBq of [^{18}F]FMISO and images were acquired at 4 hours post injection. Hypoxia was defined as TMR$_{4hr}$ greater than the average nasopharynx-to-muscle uptake in normal controls +1.96 standard deviation. Overall, 13/16 (81%) patients had increased [^{18}F]FMISO uptake: mean TMR$_{4hr}$ 1.35 (new PET) and 1.23 (conventional PET/CT). IMRT dose escalation planning simulations using both the new and conventional [^{18}F]FMISO PET images were performed in ten patients to deliver 84 Gy to the GTV$_h$. No GTV$_h$ margin expansion was applied to generate PTV$_h$. The GTV$_h$ derived from the new PET was smaller (1.5±1.6 cc) compared to that derived from conventional PET/CT (4.7±4.6 cc, P=0.002), which the authors attributed to variation in scatter fraction and spatial resolution. Superior dose distribution was achieved using the new PET data. Dose escalation was feasible in all new PET-guided plans in contrast to 9 out of 10 conventional PET plans. In comparison to the previous study by Choi *et al.*, there was a lower proportion of patients with T4 disease in this study, which may account for the difference in the number of successful dose escalations. Perhaps a more pertinent point to consider prior to the clinical implementation of any hypoxia imaging-guided dose escalation is that the GTV$_h$ volumes can vary as much as 31% solely due to the use of different scanners as demonstrated in this study. Besides that, the inherent temporal variation of any hypoxia biomarker uptake has to be taken into account as a radiotherapy plan is generated based on a set of images acquired at one time point, with a real risk of missing the hypoxic target volume over a typical fractionated treatment time of 6–7 weeks. This is supported by a [^{18}F] FMISO PET/CT reproducibility study by Nehmeh *et al.* that included 14 patients with HNSCC (82). Pretreatment [^{18}F]fluorodeoxyglucose (FDG)-PET/CT was performed for radiotherapy planning. Two sequential pretreatment [^{18}F]FMISO PET/CT scans were performed 3 days apart. Images were acquired at an average of 162 minutes post injection of 385 MBq [^{18}F]FMISO for both scans. Voxel-by-voxel image registration was performed using the CT datasets. HVs were defined using the TBR threshold of 1.2. Although relatively good correlation between the two scans was found when all voxels within the [^{18}F]FDG-derived tumour volumes were considered (average r=0.6), the correlation was much poorer when the analysis was limited to voxels with TBR ≥1.2 (r=0.3) due to the contribution of lower intensity voxels in the former analysis. The lack of stability of intratumoral high-intensity [^{18}F]FMISO distribution is a critical issue in fractionated radiotherapy treatment which may in contrast to the general belief, compromise tumour control. Hence, any biological radiotherapy dose painting treatment should be performed within the context of a prospective study to evaluate the long-term tumour control and safety data of each imaging biomarker using standardised image acquisition hardware and software before we can fully embrace it in clinical practice.

To our knowledge, there is no published data regarding treatment-induced changes in [^{18}F]FMISO PET in

NPC. Temporal changes of [18F]FMISO uptake during chemoradiation and chemotherapy in HNSCC have been assessed but no firm conclusions about the significance of these results can be made due to the small sample size in these studies (73,78).

[18F]Fluoroazomycin arabinofuranoside ([18F]FAZA)

[18F]FAZA is one of the second generation nitroimidazoles which is coupled to an arabinose sugar thus increasing its lipophilicity and subsequent clearance from non-hypoxic tissues (83). This should improve tumour-to-background uptake ratios although intratumoral accumulation of [18F]FAZA was shown to be less than that of [18F]FMISO (61). Nonetheless, another preclinical study showed that [18F]FAZA was associated with higher TBR and TMR compared to [18F]FMISO (84). [18F]FAZA TBR was shown to be maximal and stable at 2 hours post injection (85).

A few preclinical studies compared [18F]FAZA uptake with endogenous and exogenous hypoxic markers in SCC and fibrosarcoma xenografts (86-88). Overall, there were significant positive correlations observed between spatial localisation of [18F]FAZA and pimonidazole (86,87). The same group also used a different method to quantify the correlation between [18F]FAZA and hypoxia mRNA biomarkers such as GLUT1, CA-IX and lysyl oxidase (LOX) by analysing the respective uptake and transcription by weight in fragmented tissues (88). They found a strong correlation between [18F]FAZA retention and hypoxia gene expression profile. Another group compared [18F]FAZA uptake with pO_2 estimation using the OxyLite fibreoptic system which converts optical fluorescence signal intensities to pO_2 values in a rhabdomyosarcoma xenograft model (89). The group used TBaR at 3 hours post injection, whereby background was defined as a volume within the pelvic region. The group found that [18F]FAZA TBaR was lower and pO_2 was higher in the carbogen-breathing animals compared to those breathing room air. However, the correlation between the two parameters was only moderate at best (r=0.50–0.55).

There are no published studies which evaluated [18F]FAZA PET in NPC alone. The DAHANCA group evaluated the prognostic value of [18F]FAZA PET in 40 patients with HNSCC which included 3 patients with nasopharyngeal primary (90). All patients were treated with concurrent chemoradiation and the hypoxic cell sensitiser, nimorazole. All patients underwent pretreatment [18F]FAZA PET/CT and 13 had a second PET/CT which was performed during treatment. For the scan, an average of

365 MBq [18F]FAZA was injected intravenously and a static PET acquisition was undertaken at 2 hours post injection. Twenty-five (63%) patients had evidence of tumour hypoxia which was defined as TMR ≥1.4. [18F]FAZA uptake was associated with inferior DFS (60% vs. 93%, P=0.04). Seven out of 13 patients who underwent a second PET scan showed no evidence of residual [18F]FAZA uptake. The other six patients had smaller HVs within the same region as the initial PET scan, suggesting reoxygenation occurred during treatment.

Souvatzoglou et al. performed a pilot study comparing dynamic and static [18F]FAZA PET acquisition in 11 head and neck patients including one patient with NPC (91). Dynamic acquisition was performed up to 4 hours following a 315 MBq injection of [18F]FAZA. In addition, static PET was acquired at 2 and 4 hours post injection. The authors found that static [18F]FAZA imaging at 2 hours post injection provided the optimal signal-to-background ratio. The same group expanded the study (n=18) and showed that it was feasible to escalate the radiation dose to 80.5 Gy to the [18F]FAZA-defined GTV_h, which included all voxels with [18F]FAZA uptake ≥50% of background muscle SUV_{mean} (92).

A Dutch group performed four sequential [18F]FAZA PET/CT scans in six patients with stage IV head and neck cancers (93). Patients were imaged at baseline, week 1, week 2 and week 4 of chemoradiation. Fractional HV (FHV) was defined as the volume within the FDG-derived GTV with [18F]FAZA TMR ≥1.4. They found that 5 out of 6 patients had significant baseline intratumoral hypoxia (FHV >10%). FHV decreased during the course of treatment but remained relatively stable after week 2. The authors concluded that [18F]FAZA PET/CT at week 2 rather than at baseline may be the most reliable for dose escalation radiotherapy planning.

Other nitroimidazoles

Various second generation nitroimidazoles with improved pharmacokinetics and clearance properties compared to [18F]FMISO have been evaluated in head and neck cancers although their evidence in NPC is lacking. [18F]Fluoroerythronitroimidazole ([18F]FETNIM) is a hydrophilic nitroimidazole which has been studied in HNSCC (94-96). [18F]FETNIM tumour-to-mediastinum ratio was shown to have moderate correlations with GLUT1, HIF-1α and VEGF staining in non-small cell lung cancer (NSCLC) (97). The Turku group has the most experience with [18F]FETNIM PET/CT in head and neck

Page 12 of 24

Yip et al. Molecular imaging of hypoxia in NPC

cancers and they suggested that the initial [18F]FETNIM uptake is influenced by blood flow and hypoxia-specific signal is optimal at 60–90 minutes post tracer injection (94). The group further evaluated this association in a cohort of patients with HNSCC including two nasopharyngeal primaries (96). ^{15}O-labelled water ([^{15}O]H$_2$O) PET was used as a surrogate for tumour blood flow. Following completion of [^{15}O]H$_2$O PET, between 289–385 MBq of [18F]FETNIM was injected intravenously. Two image acquisition protocols were used: dynamic for 120 minutes post injection and static acquisitions at 0–20 and 80–120 minutes. [18F]FETNIM quantification was calculated using the data acquired between 90–120 minutes. Hypoxia was defined as tumour-to-plasma activity more than three standard deviations above the average normal tissue-to-plasma activity ratio which was based on this particular cohort of patients. In this study, blood flow was not associated with [18F]FETNIM FHV or tumour-to-plasma ratio. The two NPC primaries exhibited moderate intratumoral blood flow (20 and 37 mL/100 g/min) with corresponding HFV of 20% and 34%. The study found that FHV greater than the median was associated with inferior OS (P=0.036).

[18F]EF5 is an analogue of etanidazole but is more lipophilic than [18F]FMISO. Its superiority over [18F]FMISO has yet to be proven (98). The Turku group compared the prognostic significance of [18F]EF5, [18F]FDG and [^{15}O]H$_2$O PET in 22 patients with HNSCC, of whom two had nasopharyngeal primaries (99,100). Following injection of approximately 277 MBq of [18F]EF5, a static PET acquisition was performed at 3 hours post injection. A TMR >1.5 was considered to represent hypoxia. Six patients had no detectable hypoxia. The two NPC primaries exhibited some degree of hypoxia as detected by [18F]EF5 PET (maximum TMR 1.84/2.10 and HF 16/38%). None of the PET parameters were significant prognostic factor in this cohort of patients.

[18F]HX4 is very hydrophilic with rapid renal clearance (98). One study compared [18F]HX4 with [18F]FMISO PET/CT in a small cohort of patients with head and cancers (n=12) (101). Approximately 7.3 MBq/kg of [18F]FMISO and 7.6 MBq/kg of [18F]HX4 were administered on separate days. For [18F]HX4 PET, images were acquired at 1.5 hours post injection and [18F]FMISO PET was performed at 2 hours. A TMR ≥1.3 was used to define hypoxia for both tracers. There was a good correlation between [18F]HX4 with [18F]FMISO uptake (r^2=0.84). However, there was no improvement of [18F]HX4 SUV$_{max}$ and TMR over that of [18F]FMISO. Nonetheless, the

authors stated that there was lower background signal of whole-body [18F]HX4 imaging compared to [18F]FMISO. The study also evaluated the association between the uptake of the tracers and CA-IX staining in nine patients. Both tracers showed good association with CA-IX expression.

Cu-ATSM

Cu-ATSM is a lipophilic Cu(II) complex that rapidly passes through the cell membrane. Its exact retention mechanism within hypoxic cells is still unclear (102,103). All hypotheses involve the reduction of Cu(II) to Cu(I) with various intracellular reducing agents being proposed such as mitochondrial nicotinamide adenine dinucleotide (NADH) (102) and cytoplasmic reductants such as NADPH (103). It is thought that Cu-ATSM is reduced in both normoxic and hypoxic cells to the less lipophilic and unstable Cu(I)-ATSM complex. This process is reversible in the presence of oxygen, allowing the reoxidised Cu-ATSM to diffuse out of the cell. However, this is irreversible in the hypoxic environment, thus trapping the Cu(I) ions within hypoxic cells (104-106). A number of copper isotopes with varying physical half-lives can be used to label this compound: ^{60}Cu (T$_{1/2}$ =24 minutes), ^{61}Cu (T$_{1/2}$ =3.3 hours), ^{62}Cu (T$_{1/2}$ =9.7 minutes) and ^{64}Cu (T$_{1/2}$ =12.7 hours) (49). Due to very short half-life of ^{62}Cu, it has to be produced on-site in a ^{62}Zn/^{62}Cu generator (107). The choice of isotopes will depend on studied hypothesis and availability of isotopes.

The specificity of Cu-ATSM as a true hypoxia biomarker is still being debated. *Table 4* shows the studies which have evaluated the evidence in this aspect (56,61,62,108-110). The hypoxia selectivity of Cu-ATSM has been suggested to be cell line (108,111) and time dependent (56,62). This is supported by the finding that fatty acid synthase expression, a marker of tumour aggressiveness in prostate cancer, inhibited [^{64}Cu]ATSM retention in several prostate carcinoma cell lines (112). The conflicting evidence for its hypoxia selectivity may be partly attributed to all these reasons, leading to opinions that Cu-ATSM retention may not be entirely hypoxia specific but dictated by the intracellular redox potential (62,113). Despite this, Cu-ATSM uptake has been shown to be a significant prognostic factor in NSCLC, cervical and rectal cancers which could be independent of its status as a true hypoxic biomarker (114-116).

The role of Cu-ATSM PET in head and neck cancers has been studied but no published study has evaluated its

Table 4 Studies which compared Cu–ATSM uptake against pO2 measurements and hypoxia immunohistochemistry

Study	Study type	Radiotracer	Tumour type	PET parameters	Hypoxic markers	Results
Carlin et al. (61)	Preclinical	[^{64}Cu]ATSM. Images acquired at 80–90 minutes pi	Human HNSCC (SQ20b) (used in all four tracer experiments). Human colon cancer (HCT116 & HT29) (used only in [^{64}Cu]ATSM experiments)	4 tracers evaluated: [^{18}F]FMISO, [^{18}F]FAZA, [^{18}F]HX4 & [^{64}Cu]ATSM. Autoradiography	Pimonidazole, CA-IX, Hoechst 33342	Qualitative: areas of high uptake of [^{64}Cu] ATSM corresponded to regions of low Pimonidazole & CA-IX staining, and high Hoechst 33342 staining. Quantitative: negative weak correlations between [^{64}Cu]Cu-ATSM and pimonidazole (r=−0.110) & CA-IX (r=−0.158) but positive correlation with Hoechst 33342 (r=0.077)
Yuan et al. (108)	Preclinical	[^{64}Cu]ATSM. Dynamic acquisition for 1 hour pi	R3230 mammary adenocarcinoma, fibrosarcoma (FSA), 9L gliosarcoma	Autoradiography	EF5, pimonidazole, CA-IX, Hoechst 33342	Cell line dependency of [^{64}Cu]ATSM hypoxia selectivity: significant [^{64}Cu]ATSM uptake & EF5 staining correlations observed in R3230 (r=0.74±0.02) and 9L (r=0.61±0.04) tumours but not FSA (r=0.11±0.03); no spatial correlation between pimonidazole & CA-IX with [^{64}Cu]ATSM autoradiography in FSA tumours but good spatial correlation observed in R3230. Carbogen effect in FSA xenograft: EF5 staining decreased in Carbogen-breathing animals compared to air-breathing animals but no significant decrease in [^{64}Cu] ATSM uptake
O'Donoghue et al. (56)	Preclinical	[^{64}Cu]ATSM. Early acquisition: 30 min–2 hours pi and late: 16–20 hours pi	R3327-AT anaplastic prostate adenocarcinoma	Autoradiography	OxyLite fibreoptic probe which converts optical fluorescence SI to pO$_2$ values. Pimonidazole, Hoechst 33342	Late [^{64}Cu]ATSM images corresponded better to pO$_2$ measurements compared to early images. Negative correlations observed between early [^{64}Cu]ATSM uptake & pimonidazole (r=−0.76/0.77) and equivocal correlations with Hoechst 33342 (r=0.34/−0.36). Positive correlations observed between late [^{64}Cu]ATSM uptake & pimonidazole (r=0.61/0.64) and equivocal correlations with Hoechst 33342 (r=0.35/−0.11)

Table 4 (*continued*)

Table 4 (*continued*)

Study	Study type	Radiotracer	Tumour type	PET parameters	Hypoxic markers	Results
McCall et al. (109)	Preclinical	[64Cu]ATSM Dynamic acquisition for 50–90 minutes at 2 time points: 1 hour pi (early) and 18 hours pi (late)	FaDu	Autoradiography	Pimonidazole, Hoechst 33342	No correlations were noted between early & late [64Cu]ATSM and pimonidazole staining. Significant positive correlation between early [64Cu]ATSM uptake and Hoechst 33342 but not with late [64Cu]ATSM uptake
Hueting et al. (62)	Preclinical	[64Cu]ATSM & [64Cu] acetate: dynamic acquisition for 2 hours pi	EMT6 mouse mammary cell line, CaNT murine adenocarcinoma	Autoradiography	EF5	No correlation between [64Cu]ATSM/[64Cu] acetate uptake at 15 minutes with EF5. Moderate correlations between [64Cu]ATSM/[64Cu]acetate uptake at 2 hours with EF5. Good correlations between [64Cu]ATSM/[64Cu] acetate uptake at 16 hours with EF5
Tateishi et al. (110)	Clinical	[62Cu]ATSM	Gliomas (n=22)	TBaR between 30–40 minutes pi	HIF-1α	TBaR cut off 1.8 predicted for HIF-1α expression (sensitivity 92%, sensitivity 89%, AUC 0.92)

HNSCC, head and neck squamous cell carcinoma; pi, post injection; CA-IX, carbonic anhydrase-IX; HIF-1α, hypoxia-inducible factor-1α; SI, signal intensities; AUC, area under the curve; TBaR, tumour-to-background ratio.

use in NPC (*Figure 1*). A Japanese pilot study showed that a pretreatment [62Cu]ATSM SUV_{max} >5.0 was associated with inferior locoregional control following chemoradiation in 17 patients with advanced head and neck cancers (117). In a separate study, [62Cu]ATSM TMR >3.2 predicted for inferior DFS and progression-free survival (PFS) in 22 patients with head and neck malignancies (118). However, [62Cu] ATSM SUV_{max} >3.6 was associated with poorer PFS but not DFS in the same study. Grassi *et al.* assessed the prognostic role of early (1 hour post injection) and late [64Cu]ATSM PET/CT (16 hours post injection) in eleven patients with advanced head and neck malignancies, of whom one had nasopharyngeal cancer (119). No significant difference was found between early and late PET acquisitions. A [64Cu] ATSM SUV_{max} threshold of 17.8 was associated with good sensitivity (100%) but poor specificity (50%) in predicting complete response after chemoradiation with an area under the curve (AUC) of 0.7. It has to be noted that these studies included a small heterogeneous population and these results should be validated in larger studies.

Cu-ATSM guided head and neck radiotherapy planning was first considered by Chao *et al.* using [60Cu]ATSM PET/CT (120). The group used [60Cu]ATSM TMR >2.0 to define hypoxia in this study. The GTV_h was simulated to receive 80 Gy in 35 fractions without compromising normal tissue tolerances. The stability of hypoxia within head and neck tumours as depicted on Cu-ATSM PET during treatment was assessed by Nyflot *et al.* in a phase I therapeutic study evaluating the addition of bevacizumab to concurrent chemoradiation (121). All ten patients had stage IV oropharyngeal SCC and received induction bevacizumab followed by concurrent chemoradiation 3 weeks later. Patients underwent [18F]fluorothymidine (FLT), a marker of cellular proliferation, and [61Cu]ATSM PET/CT at three time points: before treatment, 3 weeks after induction bevacizumab and during week 1–2 of chemoradiation. All patients showed significant reductions in [18F]FLT SUV_{mean} and SUV_{peak} after induction bevacizumab and chemoradiation. In contrast, although there was a significant overall reduction in [61Cu]ATSM SUV_{mean} during treatment, these changes were less consistent in an individual patient basis which was similar to the preclinical findings of the heterogeneous Cu-ATSM uptake between different cell lines and xenografts.

Overall, there is very little evidence on the use of Cu-ATSM in NPC but the limited data in the head and neck cancer cohort suggests that there is potential for its use as a prognostic biomarker. Its use in radiotherapy planning
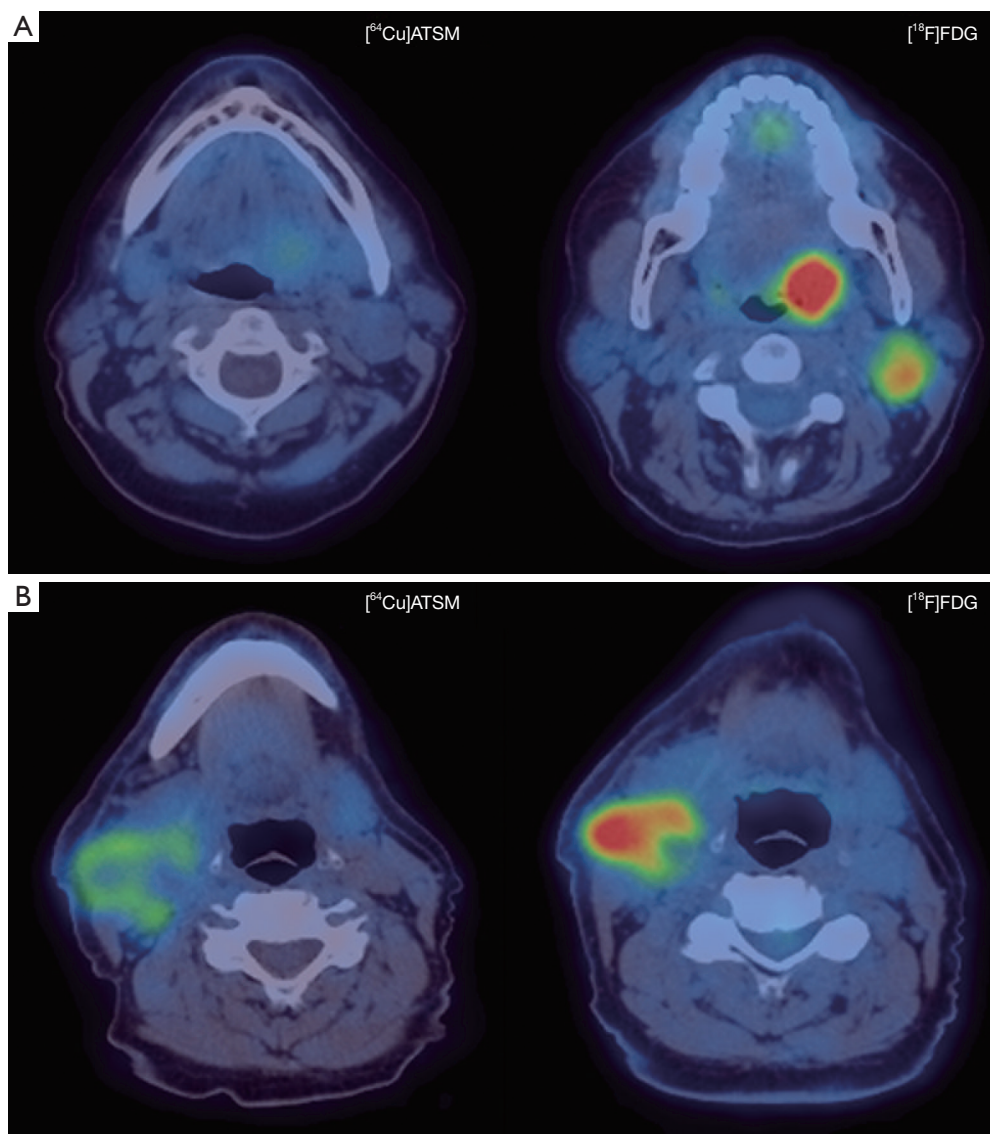
Figure 1 [^{64}Cu]ATSM PET/CT (left) and corresponding [^{18}F]FDG PET/CT (right) of an (A) oropharyngeal primary with ipsilateral cervical lymphadenopathy showing increased FDG uptake but only mild [^{64}Cu]ATSM uptake in the primary tumour and (B) enlarged FDG-avid right cervical lymph node with increased [^{64}Cu]ATSM at the periphery. Used with permission from Dr. Suh Yae-Eun and Dr. Teresa Guerrero-Urbano, Department of Clinical Oncology, Guy's & St Thomas' NHS Foundation Trust, London, UK. PET, positron emission tomography; CT, computed tomography.

is feasible but we are faced with the same difficulty as with the nitroimidazoles with regards to temporal variation in intratumoral oxygenation. In addition, the uncertainty of Cu-ATSM as a true hypoxia biomarker should ideally be resolved before it is used to direct hypoxia-targeting therapy.

Single photon emission computed tomography (SPECT)

SPECT hypoxia imaging is feasible although research into its use in the aspect has received less attention than PET in recent years. SPECT radiotracers typically have longer half-lives compared to PET tracers, permitting delayed imaging

Page 16 of 24

Yip et al. Molecular imaging of hypoxia in NPC

to be performed. The spatial resolution and detection sensitivity of SPECT are lower than PET but a SPECT scanner is cheaper compared to PET which could be an important factor in terms of cost-effectiveness in certain healthcare systems (122). Quantification of SPECT tracer uptake is also less developed compared to PET.

Iodoazomycin arabinoside (IAZA)

IAZA is a misonidazole analogue which has been proposed as an hypoxia imaging biomarker and can be coupled to iodine-123 (^{123}I) (T$_{1/2}$ =13 hours) or [125]I (T$_{1/2}$ =59 days) (123). *In vitro* study showed high ^{125}I avidity in hypoxic EMT6 cells whereas little [125]IIAZA uptake occurred in oxic cells (124). Parliament *et al.* demonstrated adequate [123]IIAZA uptake at 18–24 hours post injection in predominantly lung cancers (125). The same group went on to compare [123]IIAZA and [99mTc]hexamethylpropylenamine oxime ([99mTc]HMPAO) SPECT, a surrogate of perfusion in a separate study (n=22) which included six head and neck patients (126). They found an inverse correlation between [123]IIAZA and [99mTc]HMPAO uptakes, mainly of poorly perfused areas that corresponded to areas with increased [123]IIAZA uptake. An expanded study cohort of 52 patients which included those with head and neck cancers (n=6), small cell lung cancer (n=15), malignant gliomas (n=11) and other malignancies showed that 40% of the head and neck tumours were hypoxic, defined as TBR >1.10 (127). A similar inverse relationship between [123]IIAZA and [99mTc]HMPAO uptakes was shown except in the glioma subgroup in which none of the patients showed uptake of [123]IIAZA. This could perhaps be attributed to the presence of significant intratumoral necrosis, a common phenomenon in glioblastoma, although this information was not given to confirm this hypothesis.

HL91

[99mTc]Butylene amineoxime ([99mTc]HL91) is a single-photon-emitting radiotracer without the 2-nitroimidazole group and has greater hypoxia selectivity compared to the 2-nitroimidazole-containing tracers (128). The uptake of [99mTc]HL91 was shown to correlate with GLUT1 expression in rat mammary carcinoma xenografts (129). A small study evaluated the potential of [99mTc]HL91 SPECT in detecting locoregional recurrence in head and neck cancers (130). Nine patients with suspicious clinical recurrence were recruited and underwent conventional CT and [99mTc]HL91 SPECT. SPECT acquisition was performed at 2 and 4 hours post injection of tracer. Five patients were subsequently confirmed to have local recurrence on CT and biopsy. [99mTc]HL91 SPECT detected 3 local recurrences and 2 out of 3 nodal recurrences. The study did not find any significant difference between early and late [99mTc]HL91 tumour-to-normal tissue ratios. Based on this limited evidence, [99mTc]HL91 SPECT is unlikely to be used as a first-line imaging tool in detecting *de novo* or recurrent tumours.

Future directions

Molecular hypoxia imaging assessment in NPC is limited but we can probably extrapolate some data from the HNSCC population. There is perhaps less doubt about the significance of hypoxia as a negative prognostic and predictive factor in NPC than the actual prevalence of clinically and radiobiologically relevant hypoxia in this disease. Hence, more research should be done to ascertain the prevalence of hypoxia in NPC. A true hypoxia imaging biomarker which is not affected by tumour perfusion and blood flow, amongst other criteria as discussed before, will be the ideal clinical tool to use but such a biomarker is unlikely to exist.

The future of hypoxia assessment is likely to involve multimodality functional imaging. Simultaneous assessment of hypoxia and perfusion/blood flow will be desirable, allowing oncologists to target the predominant process contributing to hypoxia. The combined use of different functional imaging modalities such as PET, magnetic resonance imaging (MRI) and CT should be considered. CT and MRI have advanced beyond conventional anatomical imaging. Functional MRI such as blood oxygen dependent (BOLD), dynamic contrast-enhanced (DCE) and diffusion-weighted (DW) MRI can provide additional evaluation of tumour oxygenation, perfusion/ blood flow and cellular density, respectively. BOLD MRI is based on the intrinsic differential magnetic properties of oxyhaemoglobin and deoxyhaemoglobin. The paramagnetic deoxyhaemoglobin shortens the $T2^*$ of blood and increases the MR transverse relaxation rate ($R2^* = 1/T2^*$) measured using gradient echo (GRE) sequences (131). DCE-MRI evaluates the tumour enhancement characteristics before and after a fast bolus of intravenous low-molecular weight gadolinium contrast agent injection using T1-weighted spoiled GRE sequence (132). The use of DCE-MRI has been recently been evaluated in NPC with encouraging

results (133-135). DW MRI measures the rate of water Brownian motion within tissues using a pair of field gradients with varying amplitudes and gradient durations which are both summarised as *b*-values, that defocus and refocus signals of water molecules (136). Quantitative assessment is possible by acquiring images using at least two *b*-values to generate apparent diffusion coefficient (ADC) which is an average of water motion in three directions. Hypercellular tumours exhibit restricted diffusion and corresponding low ADC. Although often thought as measurement of tissue diffusivity, the DW signal attenuation is affected by both molecular diffusion and microcirculation of blood in the capillary network (137,138). Intravoxel incoherent motion (IVIM)-based analysis permits estimation of tumour perfusion and diffusivity by performing DW MRI using multiple *b*-values (usually more than 10). The measured signal attenuation acquired using low *b*-values is affected predominantly by microcapillary perfusion whereas signal attenuation at higher *b*-values is less sensitive to perfusion. IVIM-based analysis has been investigated in NPC to differentiate malignant tumours from radiation fibrosis (139) and benign tumours (140), to predict locoregional tumour staging (141) and response to neoadjuvant chemotherapy (142). Although initial results are promising, there are significant challenges to overcome before we can introduce this technique into clinical practice. Measurements of signal attenuation at low *b*-values are susceptible to signal-to-noise variations and have poor reproducibility. In addition, the optimal mathematical model to quantify perfusion and diffusion characteristics is still unclear (138). Similar to DCE-MRI, perfusion CT assesses the temporal changes in tumour attenuation after intravenous iodinated contrast administration, allowing estimation of intratumoral blood flow, blood volume and vessel permeability (143,144). Although sequential PET and functional MRI/CT can be performed on different occasions, near simultaneous acquisitions of PET and MRI/CT will be advantageous in terms of patient convenience and minimising the effect of temporal heterogeneity between scans. The introduction of PET/MRI has the potential to improve diagnostic and radiotherapy planning ability although there is still much uncertainty regarding the use of MR attenuation correction and research is still on going in this area. Nonetheless, this is an exciting prospect in hypoxia imaging particularly in NPC where the superior soft tissue definition on MRI will be clinically valuable.

Contrast-enhanced ultrasonography using microbubbles of injectable gas in a shell made up of phospholipids, proteins or polymer that remain intravascularly can be used to assess tumour perfusion (145). These microbubbles of 1–4 μm in diameter are safe for patient use. The feasibility of this method to assess perfusion in liver and nodal metastases as well as renal cell carcinoma has been shown in a few studies (146-148). Although not a direct assessment of hypoxia, contrast-enhanced ultrasonography could give additional perfusion/flow information which is related to the oxygenation status within the tumours. However, the availability of the microbubbles and the technical experience required have to be considered prior to its implementation.

Conclusions

Pathological evidence and to a lesser extent, invasive pO_2 assessment suggest that intratumoral hypoxia exists in a proportion of nasopharyngeal tumours, particularly in bulky primary and/or nodal disease. $[^{18}F]FMISO$ is the most widely studied imaging hypoxia biomarker, but its clinical use has been limited by its suboptimal pharmacokinetic properties. Newer generation nitroimidazoles and Cu-ATSM are viable alternatives although none of these tracers are without their limitations. Multimodality functional imaging with its potential to provide simultaneous information regarding perfusion, vessel permeability, tumour architecture and cellularity could herald a new paradigm in functional assessment of NPC.

Acknowledgements

Footnote

Conflicts of Interest: The authors have no conflicts of interest to declare.

Page 18 of 24

Yip et al. Molecular imaging of hypoxia in NPC

References

1. Ferlay J, Soerjomataram I, Dikshit R, et al. Cancer incidence and mortality worldwide: sources, methods and major patterns in GLOBOCAN 2012. Int J Cancer 2015;136:E359-86.

2. Chang ET, Adami HO. The enigmatic epidemiology of nasopharyngeal carcinoma. Cancer Epidemiol Biomarkers Prev 2006;15:1765-77.

3. Chua ML, Wee JT, Hui EP, et al. Nasopharyngeal carcinoma. Lancet 2016;387:1012-24.

4. Lee AW, Ng WT, Chan YH, et al. The battle against nasopharyngeal cancer. Radiother Oncol 2012;104:272-8.

5. Barnes L, Eveson J, Reichart P, et al. editors. Pathology and Genetics of Head and Neck Tumours. Lyon: IARC Press, 2005.

6. Raab-Traub N. Epstein-Barr virus in the pathogenesis of NPC. Semin Cancer Biol 2002;12:431-41.

7. Tsao SW, Tramoutanis G, Dawson CW, et al. The significance of LMP1 expression in nasopharyngeal carcinoma. Semin Cancer Biol 2002;12:473-87.

8. Tan T, Lim WT, Fong KW, et al. Concurrent chemo-radiation with or without induction gemcitabine, Carboplatin, and Paclitaxel: a randomized, phase 2/3 trial in locally advanced nasopharyngeal carcinoma. Int J Radiat Oncol Biol Phys 2015;91:952-60.

9. Lee AW, Ngan RK, Tung SY, et al. Preliminary results of trial NPC-0501 evaluating the therapeutic gain by changing from concurrent-adjuvant to induction-concurrent chemoradiotherapy, changing from fluorouracil to capecitabine, and changing from conventional to accelerated radiotherapy fractionation in patients with locoregionally advanced nasopharyngeal carcinoma. Cancer 2015;121:1328-38.

10. Nordsmark M, Overgaard J. Tumor hypoxia is independent of hemoglobin and prognostic for loco-regional tumor control after primary radiotherapy in advanced head and neck cancer. Acta Oncol 2004;43:396-403.

11. Nordsmark M, Overgaard M, Overgaard J. Pretreatment oxygenation predicts radiation response in advanced squamous cell carcinoma of the head and neck. Radiother Oncol 1996;41:31-9.

12. Vaupel P, Thews O, Hoeckel M. Treatment resistance of solid tumors: role of hypoxia and anemia. Med Oncol 2001;18:243-59.

13. Höckel M, Vaupel P. Tumor hypoxia: definitions and current clinical, biologic, and molecular aspects. J Natl Cancer Inst 2001;93:266-76.

14. Vaupel P, Hockel M, Mayer A. Detection and characterization of tumor hypoxia using pO2 histography. Antioxid Redox Signal 2007;9:1221-35.

15. Carreau A, El Hafny-Rahbi B, Matejuk A, et al. Why is the partial oxygen pressure of human tissues a crucial parameter? Small molecules and hypoxia. J Cell Mol Med 2011;15:1239-53.

16. Becker A, Hansgen G, Richter C, et al. Oxygenation status of squamous cell carcinoma of the head and neck: comparison of primary tumors, their neck node metastases and normal tissue. Strahlenther Onkol 1998;174:484-6.

17. Becker A, Hansgen G, Bloching M, et al. Oxygenation of squamous cell carcinoma of the head and neck: comparison of primary tumors, neck node metastases, and normal tissue. Int J Radiat Oncol Biol Phys 1998;42:35-41.

18. Adam MF, Gabalski EC, Bloch DA, et al. Tissue oxygen distribution in head and neck cancer patients. Head Neck 1999;21:146-53.

19. Nordsmark M, Bentzen SM, Overgaard J. Measurement of human tumour oxygenation status by a polarographic needle electrode. An analysis of inter- and intratumour heterogeneity. Acta Oncol 1994;33:383-9.

20. Dunst J, Stadler P, Becker A, et al. Tumor volume and tumor hypoxia in head and neck cancers. The amount of the hypoxic volume is important. Strahlenther Onkol 2003;179:521-6.

21. Brizel DM, Sibley GS, Prosnitz LR, et al. Tumor hypoxia adversely affects the prognosis of carcinoma of the head and neck. Int J Radiat Oncol Biol Phys 1997;38:285-9.

22. Brizel DM, Dodge RK, Clough RW, et al. Oxygenation of head and neck cancer: changes during radiotherapy and impact on treatment outcome. Radiother Oncol 1999;53:113-7.

23. Rudat V, Stadler P, Becker A, et al. Predictive value of the tumor oxygenation by means of pO2 histography in patients with advanced head and neck cancer. Strahlenther Onkol 2001;177:462-8.

24. Nordsmark M, Bentzen SM, Rudat V, et al. Prognostic value of tumor oxygenation in 397 head and neck tumors after primary radiation therapy. An international multi-center study. Radiother Oncol 2005;77:18-24.

25. Le QT, Kovacs MS, Dorie MJ, et al. Comparison of the comet assay and the oxygen microelectrode for measuring tumor oxygenation in head-and-neck cancer patients. Int J Radiat Oncol Biol Phys 2003;56:375-83.

26. Sung FL, Hui EP, Tao Q, et al. Genome-wide expression analysis using microarray identified complex signaling pathways modulated by hypoxia in nasopharyngeal

carcinoma. Cancer Lett 2007;253:74-88.

27. Rittling SR, Chambers AF. Role of osteopontin in tumour progression. Br J Cancer 2004;90:1877-81.

28. Le QT, Sutphin PD, Raychaudhuri S, Yu SC, et al. Identification of osteopontin as a prognostic plasma marker for head and neck squamous cell carcinomas. Clin Cancer Res 2003;9:59-67.

29. Koopmann J, Fedarko NS, Jain A, et al. Evaluation of osteopontin as biomarker for pancreatic adenocarcinoma. Cancer Epidemiol Biomarkers Prev 2004;13:487-91.

30. Nordsmark M, Eriksen JG, Gebski V, et al. Differential risk assessments from five hypoxia specific assays: The basis for biologically adapted individualized radiotherapy in advanced head and neck cancer patients. Radiother Oncol 2007;83:389-97.

31. Said HM, Katzer A, Flentje M, et al. Response of the plasma hypoxia marker osteopontin to in vitro hypoxia in human tumor cells. Radiother Oncol 2005;76:200-5.

32. Lukacova S, Overgaard J, Alsner J, et al. Strain and tumour specific variations in the effect of hypoxia on osteopontin levels in experimental models. Radiother Oncol 2006;80:165-71.

33. Petrik D, Lavori PW, Cao H, et al. Plasma osteopontin is an independent prognostic marker for head and neck cancers. J Clin Oncol 2006;24:5291-7.

34. Sørensen BS, Alsner J, Overgaard J, et al. Hypoxia induced expression of endogenous markers in vitro is highly influenced by pH. Radiother Oncol 2007;83:362-6.

35. Koritzinsky M, Seigneuric R, Magagnin MG, et al. The hypoxic proteome is influenced by gene-specific changes in mRNA translation. Radiother Oncol 2005;76:177-86.

36. Xueguan L, Xiaoshen W, Yongsheng Z, et al. Hypoxia inducible factor-1 alpha and vascular endothelial growth factor expression are associated with a poor prognosis in patients with nasopharyngeal carcinoma receiving radiotherapy with carbogen and nicotinamide. Clin Oncol (R Coll Radiol) 2008;20:606-12.

37. Hui EP, Chan AT, Pezzella F, et al. Coexpression of hypoxia-inducible factors 1alpha and 2alpha, carbonic anhydrase IX, and vascular endothelial growth factor in nasopharyngeal carcinoma and relationship to survival. Clin Cancer Res 2002;8:2595-604.

38. Kitagawa N, Kondo S, Wakisaka N, et al. Expression of seven-in-absentia homologue 1 and hypoxia-inducible factor 1 alpha: novel prognostic factors of nasopharyngeal carcinoma. Cancer Lett 2013;331:52-7.

39. Wan XB, Fan XJ, Huang PY, et al. Aurora-A activation, correlated with hypoxia-inducible factor-1alpha, promotes radiochemoresistance and predicts poor outcome for nasopharyngeal carcinoma. Cancer Sci 2012;103:1586-94.

40. Shou Z, Lin L, Liang J, et al. Expression and prognosis of FOXO3a and HIF-1alpha in nasopharyngeal carcinoma. J Cancer Res Clin Oncol 2012;138:585-93.

41. Guang-Wu H, Sunagawa M, Jie-En L, et al. The relationship between microvessel density, the expression of vascular endothelial growth factor (VEGF), and the extension of nasopharyngeal carcinoma. Laryngoscope 2000;110:2066-9.

42. Chan CM, Ma BB, Hui EP, et al. Cyclooxygenase-2 expression in advanced nasopharyngeal carcinoma--a prognostic evaluation and correlation with hypoxia inducible factor 1alpha and vascular endothelial growth factor. Oral Oncol 2007;43:373-8.

43. Benders AA, Tang W, Middeldorp JM, et al. Epstein-Barr virus latent membrane protein 1 is not associated with vessel density nor with hypoxia inducible factor 1 alpha expression in nasopharyngeal carcinoma tissue. Head Neck Pathol 2009;3:276-82.

44. Wong TS, Kwong DL, Sham J, et al. Elevation of plasma osteopontin level in patients with undifferentiated nasopharyngeal carcinoma. Eur J Surg Oncol 2005;31:555-8.

45. Hui EP, Sung FL, Yu BK, et al. Plasma osteopontin, hypoxia, and response to radiotherapy in nasopharyngeal cancer. Clin Cancer Res 2008;14:7080-7.

46. Forsythe JA, Jiang BH, Iyer NV, et al. Activation of vascular endothelial growth factor gene transcription by hypoxia-inducible factor 1. Mol Cell Biol 1996;16:4604-13.

47. Koukourakis MI, Bentzen SM, Giatromanolaki A, et al. Endogenous markers of two separate hypoxia response pathways (hypoxia inducible factor 2 alpha and carbonic anhydrase 9) are associated with radiotherapy failure in head and neck cancer patients recruited in the CHART randomized trial. J Clin Oncol 2006;24:727-35.

48. Gong L, Zhang W, Zhou J, et al. Prognostic value of HIFs expression in head and neck cancer: a systematic review. PLoS One 2013;8:e75094.

49. Bourgeois M, Rajerison H, Guerard F, et al. Contribution of [64Cu]-ATSM PET in molecular imaging of tumour hypoxia compared to classical [18F]-MISO--a selected review. Nucl Med Rev Cent East Eur 2011;14:90-5.

50. Lee ST, Scott AM. Hypoxia positron emission tomography imaging with 18f-fluoromisonidazole. Semin Nucl Med 2007;37:451-61.

51. Gross MW, Karbach U, Groebe K, et al. Calibration of misonidazole labeling by simultaneous measurement

Page 20 of 24

Yip et al. Molecular imaging of hypoxia in NPC

of oxygen tension and labeling density in multicellular spheroids. Int J Cancer 1995;61:567-73.

52. Alauddin MM. Positron emission tomography (PET) imaging with (18)F-based radiotracers. Am J Nucl Med Mol Imaging 2012;2:55-76.

53. Michalski MH, Chen X. Molecular imaging in cancer treatment. Eur J Nucl Med Mol Imaging 2011;38:358-77.

54. Yip C, Blower PJ, Goh V, et al. Molecular imaging of hypoxia in non-small-cell lung cancer. Eur J Nucl Med Mol Imaging 2015;42:956-76.

55. Bentzen L, Keiding S, Horsman MR, et al. Assessment of hypoxia in experimental mice tumours by [18F] fluoromisonidazole PET and pO2 electrode measurements. Influence of tumour volume and carbogen breathing. Acta Oncol 2002;41:304-12.

56. O'Donoghue JA, Zanzonico P, Pugachev A, et al. Assessment of regional tumor hypoxia using 18F-fluoromisonidazole and 64Cu(II)-diacetyl-bis(N4-methylthiosemicarbazone) positron emission tomography: Comparative study featuring microPET imaging, Po2 probe measurement, autoradiography, and fluorescent microscopy in the R3327-AT and FaDu rat tumor models. Int J Radiat Oncol Biol Phys 2005;61:1493-502.

57. Chang J, Wen B, Kazanzides P, et al. A robotic system for 18F-FMISO PET-guided intratumoral pO2 measurements. Med Phys 2009;36:5301-9.

58. Dubois L, Landuyt W, Haustermans K, et al. Evaluation of hypoxia in an experimental rat tumour model by [(18)F] fluoromisonidazole PET and immunohistochemistry. Br J Cancer 2004;91:1947-54.

59. Troost EG, Laverman P, Kaanders JH, et al. Imaging hypoxia after oxygenation-modification: comparing [18F]FMISO autoradiography with pimonidazole immunohistochemistry in human xenograft tumors. Radiother Oncol 2006;80:157-64.

60. Troost EG, Laverman P, Philippens ME, et al. Correlation of [18F]FMISO autoradiography and pimonidazole [corrected] immunohistochemistry in human head and neck carcinoma xenografts. Eur J Nucl Med Mol Imaging 2008;35:1803-11.

61. Carlin S, Zhang H, Reese M, et al. A comparison of the imaging characteristics and microregional distribution of 4 hypoxia PET tracers. J Nucl Med 2014;55:515-21.

62. Hueting R, Kersemans V, Cornelissen B, et al. A comparison of the behavior of (64)Cu-acetate and (64)Cu-ATSM in vitro and in vivo. J Nucl Med 2014;55:128-34.

63. Zimny M, Gagel B, DiMartino E, et al. FDG--a marker of tumour hypoxia? A comparison with [18F]

fluoromisonidazole and pO2-polarography in metastatic head and neck cancer. Eur J Nucl Med Mol Imaging 2006;33:1426-31.

64. Gagel B, Piroth M, Pinkawa M, et al. pO polarography, contrast enhanced color duplex sonography (CDS), [18F] fluoromisonidazole and [18F] fluorodeoxyglucose positron emission tomography: validated methods for the evaluation of therapy-relevant tumor oxygenation or only bricks in the puzzle of tumor hypoxia? BMC Cancer 2007;7:113.

65. Mortensen LS, Buus S, Nordsmark M, et al. Identifying hypoxia in human tumors: A correlation study between 18F-FMISO PET and the Eppendorf oxygen-sensitive electrode. Acta Oncol 2010;49:934-40.

66. Cherk MH, Foo SS, Poon AM, et al. Lack of correlation of hypoxic cell fraction and angiogenesis with glucose metabolic rate in non-small cell lung cancer assessed by 18F-Fluoromisonidazole and 18F-FDG PET. J Nucl Med 2006;47:1921-6.

67. Norikane T, Yamamoto Y, Maeda Y, et al. Correlation of (18)F-fluoromisonidazole PET findings with HIF-1alpha and p53 expressions in head and neck cancer: comparison with (18)F-FDG PET. Nucl Med Commun 2014;35:30-5.

68. Sato J, Kitagawa Y, Yamazaki Y, et al. 18F-fluoromisonidazole PET uptake is correlated with hypoxia-inducible factor-1alpha expression in oral squamous cell carcinoma. J Nucl Med 2013;54:1060-5.

69. Kawai N, Lin W, Cao WD, et al. Correlation between (1)(8)F-fluoromisonidazole PET and expression of HIF-1alpha and VEGF in newly diagnosed and recurrent malignant gliomas. Eur J Nucl Med Mol Imaging 2014;41:1870-8.

70. Peeters SG, Zegers CM, Yaromina A, Current preclinical and clinical applications of hypoxia PET imaging using 2-nitroimidazoles. Q J Nucl Med Mol Imaging 2015;59:39-57.

71. Yeh SH, Liu RS, Wu LC, et al. Fluorine-18 fluoromisonidazole tumour to muscle retention ratio for the detection of hypoxia in nasopharyngeal carcinoma. Eur J Nucl Med 1996;23:1378-83.

72. Eschmann SM, Paulsen F, Reimold M, et al. Prognostic impact of hypoxia imaging with 18F-misonidazole PET in non-small cell lung cancer and head and neck cancer before radiotherapy. J Nucl Med 2005;46:253-60.

73. Eschmann SM, Paulsen F, Bedeshem C, et al. Hypoxia-imaging with (18)F-Misonidazole and PET: changes of kinetics during radiotherapy of head-and-neck cancer. Radiother Oncol 2007;83:406-10.

74. Rajendran JG, Schwartz DL, O'Sullivan J, et al. Tumor

hypoxia imaging with [F-18] fluoromisonidazole positron emission tomography in head and neck cancer. Clin Cancer Res 2006;12:5435-41.

75. Zips D, Zophel K, Abolmaali N, et al. Exploratory prospective trial of hypoxia-specific PET imaging during radiochemotherapy in patients with locally advanced head-and-neck cancer. Radiother Oncol 2012;105:21-8.

76. Rischin D, Hicks RJ, Fisher R, et al. Prognostic significance of [18F]-misonidazole positron emission tomography-detected tumor hypoxia in patients with advanced head and neck cancer randomly assigned to chemoradiation with or without tirapazamine: a substudy of Trans-Tasman Radiation Oncology Group Study 98.02. J Clin Oncol 2006;24:2098-104.

77. Lee N, Nehmeh S, Schoder H, et al. Prospective trial incorporating pre-/mid-treatment [18F]-misonidazole positron emission tomography for head-and-neck cancer patients undergoing concurrent chemoradiotherapy. Int J Radiat Oncol Biol Phys 2009;75:101-8.

78. Yamane T, Kikuchi M, Shinohara S, et al. Reduction of [(18)F]fluoromisonidazole uptake after neoadjuvant chemotherapy for head and neck squamous cell carcinoma. Mol Imaging Biol 2011;13:227-31.

79. Liu RS, Yen SH, Chang CP, et al. The Prognostic Value of [F-18] Fluoromisonidazole in Patients with Nasopharyngeal Carcinoma Receiving Radiation and Concurrent Chemotherapy. Clin Positron Imaging 1998;1:245.

80. Choi W, Lee SW, Park SH, et al. Planning study for available dose of hypoxic tumor volume using fluorine-18-labeled fluoromisonidazole positron emission tomography for treatment of the head and neck cancer. Radiother Oncol 2010;97:176-82.

81. Yasuda K, Onimaru R, Okamoto S, et al. [18F] fluoromisonidazole and a new PET system with semiconductor detectors and a depth of interaction system for intensity modulated radiation therapy for nasopharyngeal cancer. Int J Radiat Oncol Biol Phys 2013;85:142-7.

82. Nehmeh SA, Lee NY, Schroder H, et al. Reproducibility of intratumor distribution of (18)F-fluoromisonidazole in head and neck cancer. Int J Radiat Oncol Biol Phys 2008;70:235-42.

83. Kumar P, Stypinski D, Xia H, et al. Fluoroazomycin arabinoside (FAZA): synthesis, 2H and 3H-labelling and preliminary biological evaluation of a novel 2-nitroimidazole marker of tissue hypoxia. J Labelled Compd Radiopharm 1999;42:3-16.

84. Piert M, Machulla HJ, Picchio M, et al. Hypoxia-specific tumor imaging with 18F-fluoroazomycin arabinoside. J Nucl Med 2005;46:106-13.

85. Peeters SG, Zegers CM, Lieuwes NG, et al. A comparative study of the hypoxia PET tracers [(1)(8)F]HX4, [(1)(8)F] FAZA, and [(1)(8)F]FMISO in a preclinical tumor model. Int J Radiat Oncol Biol Phys 2015;91:351-9.

86. Busk M, Horsman MR, Jakobsen S, et al. Imaging hypoxia in xenografted and murine tumors with 18F-fluoroazomycin arabinoside: a comparative study involving microPET, autoradiography, PO2-polarography, and fluorescence microscopy. Int J Radiat Oncol Biol Phys 2008;70:1202-12.

87. Busk M, Mortensen LS, Nordsmark M, et al. PET hypoxia imaging with FAZA: reproducibility at baseline and during fractionated radiotherapy in tumour-bearing mice. Eur J Nucl Med Mol Imaging 2013;40:186-97.

88. Busk M, Toustrup K, Sorensen BS, et al. In vivo identification and specificity assessment of mRNA markers of hypoxia in human and mouse tumors. BMC Cancer 2011;11:63.

89. Tran LB, Bol A, Labar D, et al. Hypoxia imaging with the nitroimidazole 18F-FAZA PET tracer: a comparison with OxyLite, EPR oximetry and 19F-MRI relaxometry. Radiother Oncol 2012;105:29-35.

90. Mortensen LS, Johansen J, Kallehauge J, et al. FAZA PET/CT hypoxia imaging in patients with squamous cell carcinoma of the head and neck treated with radiotherapy: results from the DAHANCA 24 trial. Radiother Oncol 2012;105:14-20.

91. Souvatzoglou M, Grosu AL, Roper B, et al. Tumour hypoxia imaging with [18F]FAZA PET in head and neck cancer patients: a pilot study. Eur J Nucl Med Mol Imaging 2007;34:1566-75.

92. Grosu AL, Souvatzoglou M, Roper B, et al. Hypoxia imaging with FAZA-PET and theoretical considerations with regard to dose painting for individualization of radiotherapy in patients with head and neck cancer. Int J Radiat Oncol Biol Phys 2007;69:541-51.

93. Bollineni VR, Koole MJ, Pruim J, et al. Dynamics of tumor hypoxia assessed by 18F-FAZA PET/CT in head and neck and lung cancer patients during chemoradiation: possible implications for radiotherapy treatment planning strategies. Radiother Oncol 2014;113:198-203.

94. Lehtiö K, Oikonen V, Gronroos T, et al. Imaging of blood flow and hypoxia in head and neck cancer: initial evaluation with [(15)O]H(2)O and [(18)F]fluoroerythronitroimidazole PET. J Nucl Med 2001;42:1643-52.

Page 22 of 24

Yip et al. Molecular imaging of hypoxia in NPC

95. Lehtiö K, Oikonen V, Nyman S, et al. Quantifying tumour hypoxia with fluorine-18 fluoroerythronitroimidazole ([18F]FETNIM) and PET using the tumour to plasma ratio. Eur J Nucl Med Mol Imaging 2003;30:101-8.

96. Lehtiö K, Eskola O, Viljanen T, et al. Imaging perfusion and hypoxia with PET to predict radiotherapy response in head-and-neck cancer. Int J Radiat Oncol Biol Phys 2004;59:971-82.

97. Hu M, Xing L, Mu D, et al. Hypoxia imaging with 18F-fluoroerythronitroimidazole integrated PET/CT and immunohistochemical studies in non-small cell lung cancer. Clin Nucl Med 2013;38:591-6.

98. Horsman MR, Mortensen LS, Petersen JB, et al. Imaging hypoxia to improve radiotherapy outcome. Nat Rev Clin Oncol 2012;9:674-87.

99. Komar G, Seppanen M, Eskola O, et al. 18F-EF5: a new PET tracer for imaging hypoxia in head and neck cancer. J Nucl Med 2008;49:1944-51.

100. Komar G, Lehtio K, Seppanen M, et al. Prognostic value of tumour blood flow, [(1)(8)F]EF5 and [(1)(8)F]FDG PET/CT imaging in patients with head and neck cancer treated with radiochemotherapy. Eur J Nucl Med Mol Imaging 2014;41:2042-50.

101. Chen L, Zhang Z, Kolb HC, et al. (1)(8)F-HX4 hypoxia imaging with PET/CT in head and neck cancer: a comparison with (1)(8)F-FMISO. Nucl Med Commun 2012;33:1096-102.

102. Fujibayashi Y, Taniuchi H, Yonekura Y, et al. Copper-62-ATSM: a new hypoxia imaging agent with high membrane permeability and low redox potential. J Nucl Med 1997;38:1155-60.

103. Obata A, Yoshimi E, Waki A, et al. Retention mechanism of hypoxia selective nuclear imaging/radiotherapeutic agent cu-diacetyl-bis(N4-methylthiosemicarbazone) (Cu-ATSM) in tumor cells. Ann Nucl Med 2001;15:499-504.

104. Holland JP, Barnard PJ, Collison D, et al. Spectroelectrochemical and computational studies on the mechanism of hypoxia selectivity of copper radiopharmaceuticals. Chemistry 2008;14:5890-907.

105. Dearling JL, Packard AB. Some thoughts on the mechanism of cellular trapping of Cu(II)-ATSM. Nucl Med Biol 2010;37:237-43.

106. Maurer RI, Blower PJ, Dilworth JR, et al. Studies on the mechanism of hypoxic selectivity in copper bis(thiosemicarbazone) radiopharmaceuticals. J Med Chem 2002;45:1420-31.

107. Wong TZ, Lacy JL, Petry NA, et al. PET of hypoxia and perfusion with 62Cu-ATSM and 62Cu-PTSM

using a 62Zn/62Cu generator. AJR Am J Roentgenol 2008;190:427-32.

108. Yuan H, Schroeder T, Bowsher JE, Intertumoral differences in hypoxia selectivity of the PET imaging agent 64Cu(II)-diacetyl-bis(N4-methylthiosemicarbazone). J Nucl Med 2006;47:989-98.

109. McCall KC, Humm JL, Bartlett R, et al. Copper-64-diacetyl-bis(N(4)-methylthiosemicarbazone) pharmacokinetics in FaDu xenograft tumors and correlation with microscopic markers of hypoxia. Int J Radiat Oncol Biol Phys 2012;84:e393-9.

110. Tateishi K, Tateishi U, Sato M, et al. Application of 62Cu-diacetyl-bis (N4-methylthiosemicarbazone) PET imaging to predict highly malignant tumor grades and hypoxia-inducible factor-1alpha expression in patients with glioma. AJNR Am J Neuroradiol 2013;34:92-9.

111. Burgman P, O'Donoghue JA, Lewis JS, et al. Cell line-dependent differences in uptake and retention of the hypoxia-selective nuclear imaging agent Cu-ATSM. Nucl Med Biol 2005;32:623-30.

112. Vāvere AL, Lewis JS. Examining the relationship between Cu-ATSM hypoxia selectivity and fatty acid synthase expression in human prostate cancer cell lines. Nucl Med Biol 2008;35:273-9.

113. Colombié M, Gouard S, Frindel M, et al. Focus on the Controversial Aspects of (64)Cu-ATSM in Tumoral Hypoxia Mapping by PET Imaging. Front Med (Lausanne) 2015;2:58.

114. Dehdashti F, Grigsby PW, Mintun MA, et al. Assessing tumor hypoxia in cervical cancer by positron emission tomography with 60Cu-ATSM: relationship to therapeutic response-a preliminary report. Int J Radiat Oncol Biol Phys 2003;55:1233-8.

115. Dietz DW, Dehdashti F, Grigsby PW, et al. Tumor hypoxia detected by positron emission tomography with 60Cu-ATSM as a predictor of response and survival in patients undergoing Neoadjuvant chemoradiotherapy for rectal carcinoma: a pilot study. Dis Colon Rectum 2008;51:1641-8.

116. Dehdashti F, Mintun MA, Lewis JS, et al. In vivo assessment of tumor hypoxia in lung cancer with 60Cu-ATSM. Eur J Nucl Med Mol Imaging 2003;30:844-50.

117. Minagawa Y, Shizukuishi K, Koike I, et al. Assessment of tumor hypoxia by 62Cu-ATSM PET/CT as a predictor of response in head and neck cancer: a pilot study. Ann Nucl Med 2011;25:339-45.

118. Sato Y, Tsujikawa T, Oh M, et al. Assessing tumor hypoxia in head and neck cancer by PET with (6)(2)Cu-diacetyl-

bis(N(4)-methylthiosemicarbazone). Clin Nucl Med 2014;39:1027-32.

119. Grassi I, Nanni C, Cicoria G, et al. Usefulness of 64Cu-ATSM in head and neck cancer: a preliminary prospective study. Clin Nucl Med 2014;39:e59-63.

120. Chao KS, Bosch WR, Mutic S, et al. A novel approach to overcome hypoxic tumor resistance: Cu-ATSM-guided intensity-modulated radiation therapy. Int J Radiat Oncol Biol Phys 2001;49:1171-82.

121. Nyflot MJ, Kruser TJ, Traynor AM, et al. Phase 1 trial of bevacizumab with concurrent chemoradiation therapy for squamous cell carcinoma of the head and neck with exploratory functional imaging of tumor hypoxia, proliferation, and perfusion. Int J Radiat Oncol Biol Phys 2015;91:942-51.

122. Rahmim A, Zaidi H. PET versus SPECT: strengths, limitations and challenges. Nucl Med Commun 2008;29:193-207.

123. Mees G, Dierckx R, Vangestel C, et al. Molecular imaging of hypoxia with radiolabelled agents. Eur J Nucl Med Mol Imaging 2009;36:1674-86.

124. Mannan RH, Somayaji VV, Lee J, et al. Radioiodinated 1-(5-iodo-5-deoxy-beta-D-arabinofuranosyl)-2-nitroimidazole (iodoazomycin arabinoside: IAZA): a novel marker of tissue hypoxia. J Nucl Med 1991;32:1764-70.

125. Parliament MB, Chapman JD, Urtasun RC, et al. Non-invasive assessment of human tumour hypoxia with 123I-iodoazomycin arabinoside: preliminary report of a clinical study. Br J Cancer 1992;65:90-5.

126. Groshar D, McEwan AJ, Parliament MB, et al. Imaging tumor hypoxia and tumor perfusion. J Nucl Med 1993;34:885-8.

127. Urtasun RC, Parliament MB, McEwan AJ, et al. Measurement of hypoxia in human tumours by non-invasive spect imaging of iodoazomycin arabinoside. Br J Cancer Suppl 1996;27:S209-12.

128. Ballinger JR, Kee JW, Rauth AM. In vitro and in vivo evaluation of a technetium-99m-labeled 2-nitroimidazole (BMS181321) as a marker of tumor hypoxia. J Nucl Med 1996;37:1023-31.

129. Yutani K, Kusuoka H, Fukuchi K, et al. Applicability of 99mTc-HL91, a putative hypoxic tracer, to detection of tumor hypoxia. J Nucl Med 1999;40:854-61.

130. Van De Wiele C, Versijpt J, Dierckx RA, et al. 99Tc(m) labelled HL91 versus computed tomography and biopsy for the visualization of tumour recurrence of squamous head and neck carcinoma. Nucl Med Commun 2001;22:269-75.

131. Barrett T, Brechbiel M, Bernardo M, et al. MRI of tumor angiogenesis. J Magn Reson Imaging 2007;26:235-49.

132. Jackson A, O'Connor JP, Parker GJ, et al. Imaging tumor vascular heterogeneity and angiogenesis using dynamic contrast-enhanced magnetic resonance imaging. Clin Cancer Res 2007;13:3449-59.

133. Liao WH, Yang LF, Liu XY, et al. DCE-MRI assessment of the effect of Epstein-Barr virus-encoded latent membrane protein-1 targeted DNAzyme on tumor vasculature in patients with nasopharyngeal carcinomas. BMC Cancer 2014;14:835.

134. Zheng D, Chen Y, Chen Y, et al. Dynamic contrast-enhanced MRI of nasopharyngeal carcinoma: a preliminary study of the correlations between quantitative parameters and clinical stage. J Magn Reson Imaging 2014;39:940-8.

135. Zheng D, Chen Y, Liu X, et al. Early response to chemoradiotherapy for nasopharyngeal carcinoma treatment: Value of dynamic contrast-enhanced 3.0 T MRI. J Magn Reson Imaging 2015;41:1528-40.

136. Koh DM, Collins DJ. Diffusion-weighted MRI in the body: applications and challenges in oncology. AJR Am J Roentgenol 2007;188:1622-35.

137. Le Bihan D, Breton E, Lallemand D, et al. Separation of diffusion and perfusion in intravoxel incoherent motion MR imaging. Radiology 1988;168:497-505.

138. Koh DM, Collins DJ, Orton MR. Intravoxel incoherent motion in body diffusion-weighted MRI: reality and challenges. AJR Am J Roentgenol 2011;196:1351-61.

139. Lai V, Li X, Lee VH, et al. Intravoxel incoherent motion MR imaging: comparison of diffusion and perfusion characteristics between nasopharyngeal carcinoma and post-chemoradiation fibrosis. Eur Radiol 2013;23:2793-801.

140. Zhang SX, Jia QJ, Zhang ZP, et al. Intravoxel incoherent motion MRI: emerging applications for nasopharyngeal carcinoma at the primary site. Eur Radiol 2014;24:1998-2004.

141. Lai V, Li X, Lee VH, et al. Nasopharyngeal carcinoma: comparison of diffusion and perfusion characteristics between different tumour stages using intravoxel incoherent motion MR imaging. Eur Radiol 2014;24:176-83.

142. Xiao Y, Pan J, Chen Y, et al. Intravoxel Incoherent Motion-Magnetic Resonance Imaging as an Early Predictor of Treatment Response to Neoadjuvant Chemotherapy in Locoregionally Advanced Nasopharyngeal Carcinoma. Medicine (Baltimore) 2015;94:e973.

143. Jin G, Su D, Liu L, et al. The accuracy of computed tomographic perfusion in detecting recurrent

Page 24 of 24

Yip et al. Molecular imaging of hypoxia in NPC

nasopharyngeal carcinoma after radiation therapy. J Comput Assist Tomogr 2011;35:26-30.

144. Su D, Jin G, Xie D, et al. Identification of local recurrence and radiofibrosis by computed tomography perfusion on nasopharyngeal carcinoma after radiotherapy. Can Assoc Radiol J 2010;61:265-70.

145. Wilson SR, Greenbaum LD, Goldberg BB. Contrast-enhanced ultrasound: what is the evidence and what are the obstacles? AJR Am J Roentgenol 2009;193:55-60.

146. Albrecht T, Blomley MJ, Burns PN, et al. Improved detection of hepatic metastases with pulse-inversion US

during the liver-specific phase of SHU 508A: multicenter study. Radiology 2003;227:361-70.

147. Moritz JD, Ludwig A, Oestmann JW. Contrast-enhanced color Doppler sonography for evaluation of enlarged cervical lymph nodes in head and neck tumors. AJR Am J Roentgenol 2000;174:1279-84.

148. Williams R, Hudson JM, Lloyd BA, et al. Dynamic microbubble contrast-enhanced US to measure tumor response to targeted therapy: a proposed clinical protocol with results from renal cell carcinoma patients receiving antiangiogenic therapy. Radiology 2011;260:581-90.